Journal of Ceramic Processing Research. Vol. 22, No. 4, pp. 421~424 (2021)
(Received 16 November 2020, Received in revised form 8 February 2021, Accepted 02 March 2021)
https://doi.org/10.36410/jcpr.2021.22.4.421

J O U R N A L O F
Ceramic Processing Research

Enhanced electrochemical performance of Li_3PO_4 coated $LiNi_{0.8}Co_{0.1}Mn_{0.1}O_2$ cathode materials for high-energy Li-ion batteries

Do-Young Hwang and Seung-Hwan Lee*
Department of Advanced Materials Engineering, Daejeon University, Daejeon 34520, Republic of Korea

In this paper, we successfully synthesized the Li_3PO_4 coated Ni-rich $LiNi_{0.8}Co_{0.1}Mn_{0.1}O_2$ cathode and investigated electrochemical performances and structure morphology for high-energy lithium-ion battery. The Li_3PO_4 coated Ni-rich $LiNi_{0.8}Co_{0.1}Mn_{0.1}O_2$ shows superior cation mixing and there is no significant change in morphology compared to the pristine NCM. In particular, the Li_3PO_4 coated Ni-rich $LiNi_{0.8}Co_{0.1}Mn_{0.1}O_2$ exhibits an improved rate capability of 176.5 mAh g^{-1} at 4.0 C and cyclability of 80.2% (after 80 cycles). Therefore, the Li_3PO_4 coated Ni-rich $LiNi_{0.8}Co_{0.1}Mn_{0.1}O_2$ cathode can be deemed as an effective method for next-generation Li-ion batteries.

Key words: Li_3PO_4-coated Ni-rich layered $LiNi_{0.8}Co_{0.1}Mn_{0.1}O_2$, superior cation mixing, improved electrochemical performances, Li_3PO_4 coating layer, next-generation Li-ion batteries.

Introduction

Recently, there is an increasing demand for lithium-ion batteries (LIBs) to use in electric vehicles (EVs), hybrid electric vehicles (HEVs) and energy storage systems [1, 2]. It is well known that LIBs have various advantages such as high energy, long lifespan, low price and good stability [3, 4]. Up to now, $LiCoO_2$ (LCO) is widely applied to the cathode material, since it has good reversibility and stable discharge plateau. On the other hand, LCO has severe drawbacks of high price, thermal instability and environmental damage [5].

Currently, $LiNi_xCo_yMn_{1-x-y}O_2$ has intensively investigated as a replacement for LCO. The main merits of $LiNi_xCo_yMn_{1-x-y}O_2$ are superior electrochemical performances, low price and environment friendly compared to LCO [6, 7]. In particular, high Ni content ($x > 0.8$, Ni-rich $LiNi_xCo_yMn_{1-x-y}O_2$) contributes to extraordinary reversible specific capacity. However, Ni-rich $LiNi_xCo_yMn_{1-x-y}O_2$ cathode suffers from capacity decay and inferior cyclability owing to the similar ionic radius of Ni^{2+} (0.69 Å) and Li^+ (0.76 Å) as well as gas generation reacted by chemical oxidation of the electrolyte, leading to rapid performance degradation of cathode materials during cycle [8-10]. More importantly, the physical/chemical uptakes of lithium residue (Li_2CO_3 and LiOH) on the surface cause the gelation of the cathode slurry [11]. To overcome the above-mentioned shortcomings, considerable efforts have been devoted to find a feasible solution. Surface coating has been verified to provide a protective barrier at the surface of active materials, inhibiting the direct contact between active materials and electrolyte. Various metal phosphate (MP) materials, such as MPO_4 (M = Fe, Ce, Al and Sr) [12, 13], $Mn_3(PO_4)^2$ [14] and so on, are used as the attractive coating materials for LIBs.

In this paper, we successfully synthesized the Li_3PO_4-coated $Ni_{0.8}Co_{0.1}Mn_{0.1}O_2$ (NCM) with investigation of electrochemical performances. Therefore, we can confirm that the Li_3PO_4-coated NCM can enhance electrochemical performances and stabilize the structure of cathode materials.

Experimental

Spherical NCM powders were prepared via co-precipitation method. The $NiSO_4 \cdot 6H_2O$, $CoSO_4 \cdot 7H_2O$, $MnSO_4 \cdot H_2O$, Na_2CO_3 and $NH_3 \cdot H_2O$ are used to yield precursor $Ni_{0.8}Co_{0.1}Mn_{0.1}(OH)_2$. The precursor $Ni_{0.8}Co_{0.1}Mn_{0.1}(OH)_2$ and $LiOH \cdot H_2O$ were mixed 1.05:1 molar ratio to prepare NCM. And then NCM was preheated at 450 ºC for 5 and subsequently calcined 750 ºC for 15 h under flowing oxygen. For the preparation of the Li_3PO_4-NCM (P-NCM), 0.5 g polyphosphoric acid (PPA) was mixed with 10 g dimethyl sulfoxide (DMSO) and then 5 g NCM was added 5 g. This slurry was constantly stirred for 15 min and vacuum dried at 80 ºC to completely remove the residual H_2O.

The electrochemical performance of each sample was examined by using CR2032 coin-type cells with metallic lithium as negative electrode in an argon glove box. The positive electrodes were prepared by mixing NCM powder (96 wt%), conductive carbon black (2 wt%) and polyvinylidene fluoride (PVDF) binder (2 wt%)

*Corresponding author:
Tel : +82-42-280-2414
E-mail: shlee@dju.kr

and then added appropriate amount of N-methyl-2-pyrrolidone to form slurry. Prepared slurry was coated on the aluminum foil and dried at 80 °C in a vacuum oven for 12 h. The CR2032 coin-type cells were subsequently assembled in an Ar-filled glove box. 1M $LiPF_6$ in ethylene carbonate (EC), dimethyl carbonate (DMC) and ethyl methyl carbonate (EMC) (1:1:1 in volume) were used to electrolyte.

The X-ray diffraction (Philips, X-pert PRO MPD) was used to investigate the structural properties of the samples with Cu-Kα radiation at a scanning rate of 2° min^{-1} in a range of 2θ from 10° to 70°. The field emission scanning electron microscopy (FE-SEM, Hitachi S-4800) was applied to investigate particle shape of P-NCM sample. Transmission electron microscopy (TEM, JEM-2010 JEOL) was employed to confirm the coating layer. The electrochemical performances of samples were evaluated via employing a measurement equipment (TOSCAT-3100, Toyo system).

Results and Discussion

As shown in Fig. 1(a), the X-ray diffraction (XRD) patterns present the structural properties of pristine NCM and P-NCM. The XRD patterns of P-NCM are almost the same compared to pristine NCM, suggesting that the Li_3PO_4 coating layer leads to no change of the original lattice of NCM [15]. All diffraction peaks are indexed as a typical structure of layered hexagonal α-$NaFeO_2$ structure belong to the space group *R-3m* without any impurities [16]. The two splitting of (006)/(102) and (108)/(110) peaks around 38° and 65° suggests that both samples have a well-crystallized hexagonal layered structure of NCM. Besides, the peak intensity ratio of $I_{(003)}/I_{(104)}$ is related to the degree of cation mixing, resulting from the similar ionic radius of Ni^{2+} (0.69 Å) and Li^+ (0.76 Å) at the 3a site [17]. When the $I_{(003)}/I_{(104)}$ is above 1.2, it is reported that cathode materials have superior cation disorder [18]. The $I_{(003)}/I_{(104)}$ ratio of P-NCM is 1.53, demonstrating that the Li_3PO_4 coating layer contributes to improve structural stability and electrochemical properties of NCM cathode.

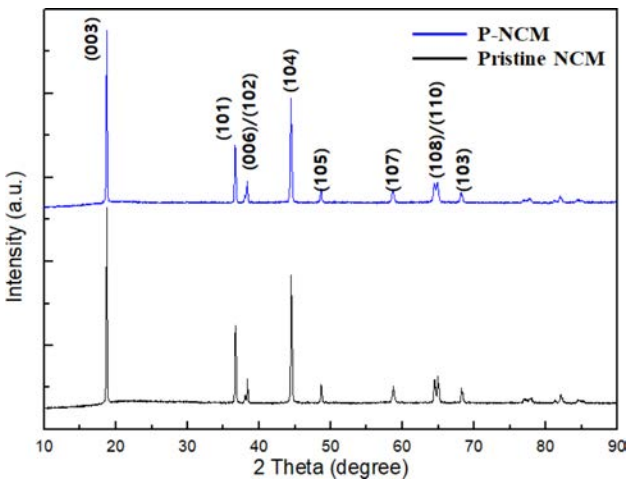

Fig. 1. XRD patterns of pristine NCM and P-NCM..

The FE-SEM images of pristine NCM and P-NCM powder can be observed in Fig. 2(a) and (b). It can be seen that both samples have a similar spherical shape with a diameter of 8-15 μm composed of primary particles with an average size of 150-200 nm. Overall, there are no significant changes between the surface shape of pristine NCM (Fig. 2(a)) and P-NCM (Fig. 2(b)). However, the surface morphology of P-NCM exhibits a somewhat rough surface morphology compared to that of pristine NCM, which is clean and smooth. Furthermore, the presence of Li_3PO_4 is proven by TEM, as shown in Fig. 2(c). It can be shown that the Li_3PO_4 coating layer has a thickness of about 60 nm. Therefore, we can confirm that the Li_3PO_4 is successfully coated over the NCM particle.

The charge-discharge curves and rate capability of both samples employed to compare the electrochemical performances, as shown in Fig. 3. The initial discharge capacities of pristine NCM and P-NCM at a rate of 0.1 C between 3.0 and 4.3 V (Fig. 3(a)) are 198.6 and 201.6 mAh g^{-1}, respectively. The rate capability (Fig. 3(b)) was performed at different discharge current rates from 0.5 C to 4.0 C. It can be observed that the capacity retention of both samples is inversely proportional to the increase of the C-rate. The pristine NCM exhibited slightly low discharge capacity as compared to that of P-NCM at low C-rates (0.5 and 1.0 C). With increasing the C-rates (2.0 and 4.0 C), the pristine NCM shows a poor rate capability (171.1 mAh g^{-1} and 159.8 mAh g^{-1}), this phenomenon occurs when direct reaction

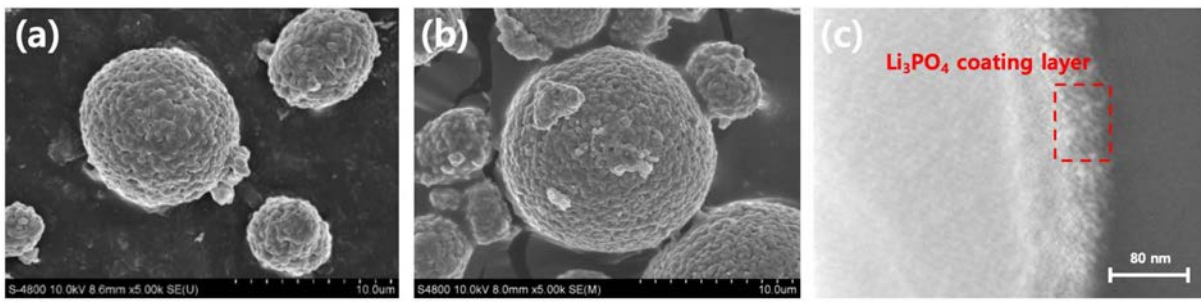

Fig. 2. FE-SEM images of (a) pristine NCM and (b) P-NCM, and (c) TEM image of P-NCM.

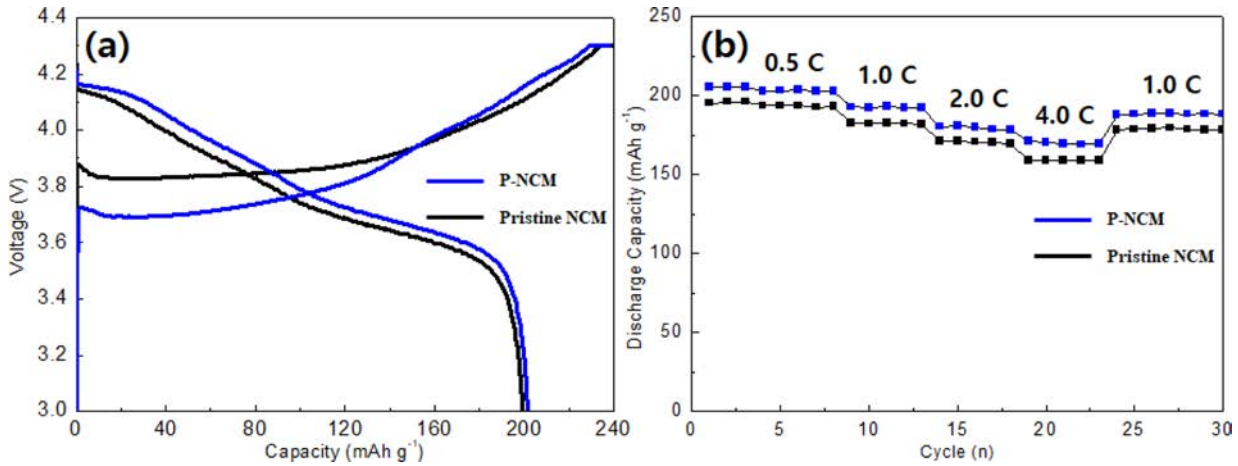

Fig. 3. Charge-discharge curves (a) and rate capability (b) of pristine NCM and P-NCM at different C-rates (0.5 C, 1.0 C, 2.0 C and 4.0 C).

between the cathode material and electrolyte which causes an increase in charge transfer resistance [19]. However, the P-NCM revealed excellent discharge capacity (176.5 mAhg^{-1} and 170.9 mAh g^{-1}) under the same condition. The significant improvement of electrochemical performance is probably derived from high conductivity of the Li_3PO_4 coating layer, which is attributed to the reduced content of insulating residual lithium compounds by li_3PO_4 coating. These observations suggest that the Li_3PO_4 coating layer of the secondary particle on the surface facilitates lithium-ion diffusion owing to superior ionic conductivity of Li_3PO_4 layer [11]. Therefore, the removal of residual lithium compounds and formation of ionic conductive Li_3PO_4 coating layer causes smooth and rapid Li transport [20].

To investigate the electrochemical performances of P-NCM, the long-term cycling performance of pristine NCM and P-NCM at a 0.5 C rate at 25 ºC in voltage range between 3.0 and 4.3 V. As shown in Fig. 4, the P-NCM has obviously better cycle stability than that of pristine NCM after 80 charge-discharge cycles. The P-NCM delivers the higher discharge capacity of 138.1 mAh g^{-1} without severe capacity decay. However, the discharge capacity of pristine NCM drastically fades to 90.2 mAh g^{-1} under the same condition. The reason is that Ni-rich NCM materials suffer from inherent problems such as unwanted side reactions with electrolyte and structural instability. However, Li_3PO_4 coating layer over the NCM particle can effectively suppress the direct contact with electrolyte as well as the oxidation of electrolyte. [20]. In particular, Fig. 4 demonstrates that the capacity retention of P-NCM is 80.2% after 80 cycles, whereas that of pristine NCM (60.7%) is slightly lower. Furthermore, it is obviously due to the influence of the Li_3PO_4 coating layer acting as a physical barrier, suppressing the formation of resistive solid electrolyte interphase (SEI) layer and the charge transfer resistance at the electrode-electrode interface between electrode and electrolyte [21]. More importantly, the coating layer of Li_3PO_4 can effectively present good electronic

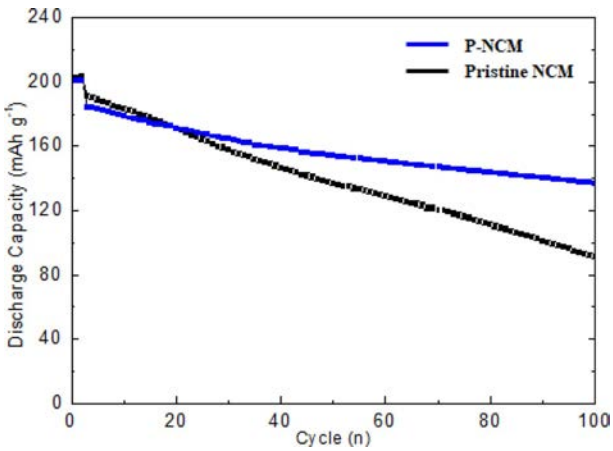

Fig. 4. Cycle performance of pristine NCM and P-NCM.

conductivity and stabilize the original layered structure against the dissolution of transition metals and undesirable reactions during cycling [22]. In additional, the Li_3PO_4 coating layer inhibits the formation of intergranular cracking, which is caused by anisotropic lattice expansion/contraction during the charge-discharge cycle [23, 24]. Therefore, surface modification of Li_3PO_4 results in significant improvement in the physical and chemical performances of the cathode materials.

Conclusions

In summary, we successfully fabricated Li_3PO_4 coating layer on the surface of Ni-rich $LiNi_{0.8}Co_{0.1}Mn_{0.1}O_2$ cathode to improve the electrochemical performances. The Li_3PO_4 coating layer on the cathode surface can improve overall structural stability, superior cyclability and excellent rate capability in contrast to the pristine NCM. These positive effects of Li_3PO_4 coating layer can be resulted from suppressing the interfacial unwanted reaction and maximizing the interfacial kinetic behavior. Therefore, it can be concluded that surface modification of Li_3PO_4 can be considered as an ideal strategy for

high-energy and long-life Ni-rich NCM cathode materials.

References

1. S.K. Jung, H. Gwon, J. Hong, K.Y. Park, D.H. Seo, H. Kim, J. Hyun, W. Yang, and K. Kang, Adv. Energy Mater. 4[1] (2014) 1300787.
2. W.S. Cho, S.M. Kim, K.W. Lee, J.H. Song, Y.N. Jo, T.E. Yim, H.T. Kim, J.S. Kim, and Y.J. Kim, Electrochim. Acta. 198 (2016) 77-83.
3. C.C. Qin, J.L. Cao, J. Chen, G.L. Dai, T.F. Wu, Y. Chen, Y.F. Tang, A.D. Li, and Y. Chen, Dalton Trans. 45[23] (2016) 9669-9675.
4. Y. Mo, L. Guo, H. Jin, B. Du, B. Cao, Y. Chen, D. Li, and Y. Chen, J. Power Sources. 448 (2020) 227439.
5. F. Lin, L.M. Markus, D. Nordlund, T.C. Weng, M.D. Asta, H.L. Xin, and M.M. Doeff, Nat. Commun. 5[1] (2014) 1-9.
6. M.S. Rad R. A. Davies, and J.D. Gale, Chem. Mater. 15[22] (2003) 4280-4286.
7. S.H. Lee, G.J. Park, S.J. Sim, B.S. Jin, and H.S. Kim, J. Alloys Compd. 791 (2019) 193-199.
8. S.J. Sim, S.H. Lee, B.S. Jin, and H.S. Kim, Sci. Rep. 9[1] (2019) 8952.
9. S. Sharifi?Asl, J. Lu, K. Amine, and R. Shahbazian?Yassar, Adv. Energy Mater. 9[22] (2019) 1900551.
10. R. Jung, P. Strobl, F. Maglia, C. Stinner, and H.A. Gastegier, J. Electrochem. Soc. 165[11] (2018) A2869-A2879.
11. J. Zhu, Y. Li, Y. Chen, T. Lei, S. Deng, T. Lei, S. Deng, and G. Cao, J. Alloys Compd 773 (2019) 112-120.
12. H. Lee, Y. Kim, Y. Hong, Y. Kim, M.G. Kim, N.S. Shin, and J. Cho, J. Electrochem. Soc. 153[4] (2006) A781-A786.
13. J. Kim, M. Noh, J. Cho, H. Kim, and K.B. Kim, J. Electrochem. Soc. 152[6] (2005) A1142-A1148.
14. W. Cho, S. Kim, K. Lee, J.H. Song, Y.N. Jo, T. Yim, H. Kim, J. Kim, and Y. Kim, Electrochim. Acta 198 (2016) 77-83.
15. S.H. Lee, S. Lee, B.S. Jin, and H.S. Kim, Sci. Rep. 9[1] (2019) 17541.
16. Y.W. Tsai, B.J. Hwang, G. Ceder, H.S. Sheu, D.G. Liu, and J.F. Lee, Chem. Mater. 17[12] (2005) 3191-3199.
17. J. Yang and Y. Xia, J. Electrochem. Soc. 163 (2016) 2665-2672.
18. C. Qin, J. Cao, J. Chen, G. Dai, T. Wu, Y. Chen, Y. Tang, A. Li, and Y. Chen, Dalton Trans. 45[23] (2016) 9669-9675.
19. S. Chen, T. He, Y. Su, Y. Lu, L. Bao, L. Chen, Q. Zhang, J. Wang, R. Chen, and F. Wu, ACS Appl. Mater. Interfaces. 9[35] (2017) 29732-29743.
20. Z. Tang, R. Wu, R. Huang, Q. Wang, and C. Chen, J. Alloys Compd. 693 (2017) 1157-1163.
21. S.H. Lee, S.J. Sim, B.S. Jin, and H.S. Kim, Mater. Lett. 270 (2020) 127615.
22. S.J. Sim, S.H. Lee, B.S. Jin, and H.S. Kim, Sci. Rep. 10 (2020) 11114.
23. P. Yan, J. Zheng, J. Liu, B. Wang, X. Cheng, Y. Zhang, X. Sun, C. Wang, and J. Zhang, Nature Energy 3[7] (2018) 600-605.
24. J.W. Seok, J. Lee, T. Rodgers, D.H. Ko, D.H. Ko, and J.H. Shim, Trans. Electr. Electron. Mater. 20[6] (2019) 548-553.